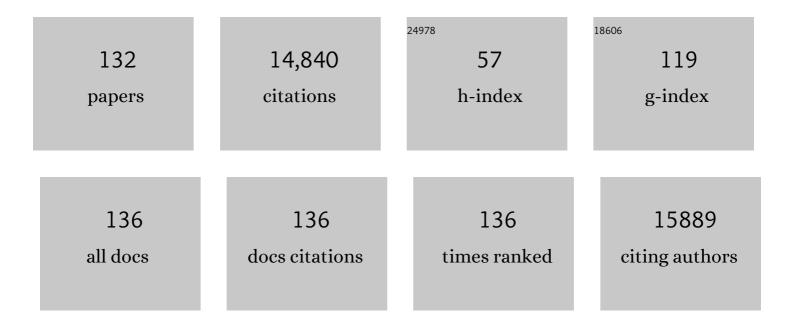
List of Publications by Year in descending order

Source: https://exaly.com/author-pdf/3415790/publications.pdf Version: 2024-02-01



#	Article	IF	CITATIONS
1	Phosphorusâ€Doped Carbon Nitride Tubes with a Layered Microâ€nanostructure for Enhanced Visibleâ€Light Photocatalytic Hydrogen Evolution. Angewandte Chemie - International Edition, 2016, 55, 1830-1834.	7.2	869
2	From coconut shell to porous graphene-like nanosheets for high-power supercapacitors. Journal of Materials Chemistry A, 2013, 1, 6462.	5.2	794
3	Nitrogen-doped graphene with high nitrogen level via a one-step hydrothermal reaction of graphene oxide with urea for superior capacitive energy storage. RSC Advances, 2012, 2, 4498.	1.7	696
4	Molecule Self-Assembly Synthesis of Porous Few-Layer Carbon Nitride for Highly Efficient Photoredox Catalysis. Journal of the American Chemical Society, 2019, 141, 2508-2515.	6.6	685
5	Integrating the active OER and HER components as the heterostructures for the efficient overall water splitting. Nano Energy, 2018, 44, 353-363.	8.2	516
6	Cost-effective large-scale synthesis of ZnO photocatalyst with excellent performance for dye photodegradation. Chemical Communications, 2012, 48, 2858.	2.2	515
7	Phosphorusâ€Modified Tungsten Nitride/Reduced Graphene Oxide as a Highâ€Performance, Nonâ€Nobleâ€Metal Electrocatalyst for the Hydrogen Evolution Reaction. Angewandte Chemie - International Edition, 2015, 54, 6325-6329.	7.2	515
8	Anionâ€Modulated HER and OER Activities of 3D Ni–Vâ€Based Interstitial Compound Heterojunctions for Highâ€Efficiency and Stable Overall Water Splitting. Advanced Materials, 2019, 31, e1901174.	11.1	479
9	Holey Reduced Graphene Oxide Coupled with an Mo ₂ N–Mo ₂ C Heterojunction for Efficient Hydrogen Evolution. Advanced Materials, 2018, 30, 1704156.	11.1	459
10	Co Nanoislands Rooted on Co–N–C Nanosheets as Efficient Oxygen Electrocatalyst for Zn–Air Batteries. Advanced Materials, 2019, 31, e1901666.	11.1	455
11	Wellâ€Ordered Largeâ€Pore Mesoporous Anatase TiO ₂ with Remarkably High Thermal Stability and Improved Crystallinity: Preparation, Characterization, and Photocatalytic Performance. Advanced Functional Materials, 2011, 21, 1922-1930.	7.8	431
12	Facile solvothermal synthesis of hierarchical flower-like Bi ₂ MoO ₆ hollow spheres as high performance visible-light driven photocatalysts. Journal of Materials Chemistry, 2011, 21, 887-892.	6.7	427
13	Interfacial Engineering of MoO ₂ â€FeP Heterojunction for Highly Efficient Hydrogen Evolution Coupled with Biomass Electrooxidation. Advanced Materials, 2020, 32, e2000455.	11.1	401
14	A Stable Bifunctional Catalyst for Rechargeable Zinc–Air Batteries: Iron–Cobalt Nanoparticles Embedded in a Nitrogenâ€Đoped 3D Carbon Matrix. Angewandte Chemie - International Edition, 2018, 57, 16166-16170.	7.2	365
15	A Promoted Charge Separation/Transfer System from Cu Single Atoms and C ₃ N ₄ Layers for Efficient Photocatalysis. Advanced Materials, 2020, 32, e2003082.	11.1	333
16	Operando Cooperated Catalytic Mechanism of Atomically Dispersed Cuâ^'N ₄ and Znâ^'N ₄ for Promoting Oxygen Reduction Reaction. Angewandte Chemie - International Edition, 2021, 60, 14005-14012.	7.2	312
17	3D hierarchical flower-like TiO2 nanostructure: morphology control and its photocatalytic property. CrystEngComm, 2011, 13, 2994.	1.3	237
18	An effective strategy for small-sized and highly-dispersed palladium nanoparticles supported on graphene with excellent performance for formic acid oxidation. Journal of Materials Chemistry, 2011, 21, 3384.	6.7	235

#	Article	IF	CITATIONS
19	Ultrathin Porous Carbon Nitride Bundles with an Adjustable Energy Band Structure toward Simultaneous Solar Photocatalytic Water Splitting and Selective Phenylcarbinol Oxidation. Angewandte Chemie - International Edition, 2021, 60, 4815-4822.	7.2	233
20	Twoâ€Dimensional Porous Molybdenum Phosphide/Nitride Heterojunction Nanosheets for pHâ€Universal Hydrogen Evolution Reaction. Angewandte Chemie - International Edition, 2021, 60, 6673-6681.	7.2	227
21	Trapping [PMo ₁₂ O ₄₀] ^{3â^'} clusters into pre-synthesized ZIF-67 toward Mo _x Co _x C particles confined in uniform carbon polyhedrons for efficient overall water splitting. Chemical Science, 2018, 9, 4746-4755.	3.7	189
22	Porous NiCoP nanosheets as efficient and stable positive electrodes for advanced asymmetric supercapacitors. Journal of Materials Chemistry A, 2018, 6, 17905-17914.	5.2	189
23	Phosphorusâ€Doped Carbon Nitride Tubes with a Layered Microâ€nanostructure for Enhanced Visibleâ€Light Photocatalytic Hydrogen Evolution. Angewandte Chemie, 2016, 128, 1862-1866.	1.6	173
24	Facile synthesis of sheet-like ZnO assembly composed of small ZnO particles for highly efficient photocatalysis. Journal of Materials Chemistry A, 2013, 1, 5700.	5.2	170
25	A facile one-pot route for the controllable growth of small sized and well-dispersed ZnO particles on GO-derived graphene. Journal of Materials Chemistry, 2012, 22, 11778.	6.7	159
26	A "MOFs plus MOFs―strategy toward Co–Mo ₂ N tubes for efficient electrocatalytic overall water splitting. Journal of Materials Chemistry A, 2018, 6, 20100-20109.	5.2	131
27	Small-sized and high-dispersed WN from [SiO ₄ (W ₃ O ₉) ₄] ^{4â^'} clusters loading on GO-derived graphene as promising carriers for methanol electro-oxidation. Energy and Environmental Science. 2014. 7. 1939-1949.	15.6	130
28	Isolated Boron and Nitrogen Sites on Porous Graphitic Carbon Synthesized from Nitrogen ontaining Chitosan for Supercapacitors. ChemSusChem, 2014, 7, 1637-1646.	3.6	128
29	Hierarchical composites of TiO2 nanowire arrays on reduced graphene oxide nanosheets with enhanced photocatalytic hydrogen evolution performance. Journal of Materials Chemistry A, 2014, 2, 4366-4374.	5.2	112
30	Hierarchical flake-like Bi2MoO6/TiO2 bilayer films for visible-light-induced self-cleaning applications. Journal of Materials Chemistry A, 2013, 1, 6961.	5.2	102
31	Cluster-like molybdenum phosphide anchored on reduced graphene oxide for efficient hydrogen evolution over a broad pH range. Chemical Communications, 2016, 52, 9530-9533.	2.2	102
32	3D hierarchical V–Ni-based nitride heterostructure as a highly efficient pH-universal electrocatalyst for the hydrogen evolution reaction. Journal of Materials Chemistry A, 2019, 7, 15823-15830.	5.2	100
33	Growth of small sized CeO2 particles in the interlayers of expanded graphite for high-performance room temperature NOx gas sensors. Journal of Materials Chemistry A, 2013, 1, 12742.	5.2	96
34	Simple Strategy for Preparation of Core Colloids Modified with Metal Nanoparticles. Journal of Physical Chemistry C, 2007, 111, 3651-3657.	1.5	87
35	In situ immobilization of ultra-fine Ag NPs onto magnetic Ag@RF@Fe3O4 core-satellite nanocomposites for the rapid catalytic reduction of nitrophenols. Water Research, 2020, 179, 115882.	5.3	87
36	A hierarchical porous carbon material from a loofah sponge network for high performance supercapacitors. RSC Advances, 2015, 5, 42430-42437.	1.7	86

#	Article	IF	CITATIONS
37	Effective Electrocatalytic Hydrogen Evolution in Neutral Medium Based on 2D MoP/MoS ₂ Heterostructure Nanosheets. ACS Applied Materials & Interfaces, 2019, 11, 25986-25995.	4.0	86
38	Magnetically separable porous graphitic carbon with large surface area as excellent adsorbents for metal ions and dye. Journal of Materials Chemistry, 2011, 21, 7232.	6.7	85
39	Vanadiumâ€Incorporated CoP ₂ with Lattice Expansion for Highly Efficient Acidic Overall Water Splitting. Angewandte Chemie - International Edition, 2022, 61, .	7.2	85
40	Controlled synthesis of thorny anatase TiO ₂ tubes for construction of Ag–AgBr/TiO ₂ composites as highly efficient simulated solar-light photocatalyst. Journal of Materials Chemistry, 2012, 22, 2081-2088.	6.7	84
41	A novel soft template strategy to fabricate mesoporous carbon/graphene composites as high-performance supercapacitor electrodes. RSC Advances, 2012, 2, 8359.	1.7	82
42	In situ growth of Bi ₂ MoO ₆ on reduced graphene oxide nanosheets for improved visible-light photocatalytic activity. CrystEngComm, 2014, 16, 842-849.	1.3	80
43	Assembly of TiO2 ultrathin nanosheets with surface lattice distortion for solar-light-driven photocatalytic hydrogen evolution. Applied Catalysis B: Environmental, 2018, 239, 317-323.	10.8	77
44	From graphite to porous graphene-like nanosheets for high rate lithium-ion batteries. Nano Research, 2015, 8, 2998-3010.	5.8	76
45	Small-sized tungsten nitride anchoring into a 3D CNT-rGO framework as a superior bifunctional catalyst for the methanol oxidation and oxygen reduction reactions. Nano Research, 2016, 9, 329-343.	5.8	75
46	Ni ₃ S ₂ Nanosheets in Situ Epitaxially Grown on Nanorods as High Active and Stable Homojunction Electrocatalyst for Hydrogen Evolution Reaction. ACS Sustainable Chemistry and Engineering, 2018, 6, 2474-2481.	3.2	72
47	Highâ€Efficient, Stable Electrocatalytic Hydrogen Evolution in Acid Media by Amorphous Fe <i>_x</i> P Coating Fe ₂ N Supported on Reduced Graphene Oxide. Small, 2018, 14, e1801717.	5.2	72
48	2D porous molybdenum nitride/cobalt nitride heterojunction nanosheets with interfacial electron redistribution for effective electrocatalytic overall water splitting. Journal of Materials Chemistry A, 2021, 9, 8620-8629.	5.2	72
49	GO-induced assembly of gelatin toward stacked layer-like porous carbon for advanced supercapacitors. Nanoscale, 2016, 8, 2418-2427.	2.8	69
50	Inorganic acid-derived hydrogen-bonded organic frameworks to form nitrogen-rich carbon nitrides for photocatalytic hydrogen evolution. Journal of Materials Chemistry A, 2017, 5, 21979-21985.	5.2	69
51	B and N isolate-doped graphitic carbon nanosheets from nitrogen-containing ion-exchanged resins for enhanced oxygen reduction. Scientific Reports, 2014, 4, 5184.	1.6	68
52	Nitrogen-doped graphene supported Pd@PdO core-shell clusters for C-C coupling reactions. Nano Research, 2014, 7, 1280-1290.	5.8	66
53	A dual-active Co-CoO heterojunction coupled with Ti3C2-MXene for highly-performance overall water splitting. Nano Research, 2022, 15, 238-247.	5.8	66
54	CoO-Mo2N hollow heterostructure for high-efficiency electrocatalytic hydrogen evolution reaction. NPG Asia Materials, 2019, 11, .	3.8	65

#	Article	IF	CITATIONS
55	A Stable Bifunctional Catalyst for Rechargeable Zinc–Air Batteries: Iron–Cobalt Nanoparticles Embedded in a Nitrogenâ€Doped 3D Carbon Matrix. Angewandte Chemie, 2018, 130, 16398-16402.	1.6	64
56	NaYF4:Er3+/Yb3+–graphene composites: preparation, upconversion luminescence, and application in dye-sensitized solar cells. Journal of Materials Chemistry, 2012, 22, 20381.	6.7	63
57	Electronic Tuning of Ni by Mo Species for Highly Efficient Hydroisomerization of <i>n</i> -Alkanes Comparable to Pt-Based Catalysts. ACS Catalysis, 2020, 10, 10449-10458.	5.5	63
58	A Floating Porous Crystalline TiO ₂ Ceramic with Enhanced Photocatalytic Performance for Wastewater Decontamination. European Journal of Inorganic Chemistry, 2013, 2013, 2411-2417.	1.0	59
59	Hierarchical Composite of Ag/AgBr Nanoparticles Supported on Bi ₂ MoO ₆ Hollow Spheres for Enhanced Visibleâ€Light Photocatalytic Performance. ChemPlusChem, 2013, 78, 117-123.	1.3	58
60	Synergistic effect of Mo ₂ N and Pt for promoted selective hydrogenation of cinnamaldehyde over Pt–Mo ₂ N/SBA-15. Catalysis Science and Technology, 2016, 6, 2403-2412.	2.1	58
61	Porous cobalt/tungsten nitride polyhedra as efficient bifunctional electrocatalysts for overall water splitting. Journal of Materials Chemistry A, 2020, 8, 22938-22946.	5.2	56
62	Inâ€Situ Fabrication of Ag/Ag ₃ PO ₄ /Graphene Triple Heterostructure Visibleâ€Light Photocatalyst through Grapheneâ€Assisted Reduction Strategy. ChemCatChem, 2013, 5, 1359-1367.	1.8	54
63	Synergism of molybdenum nitride and palladium for high-efficiency formic acid electrooxidation. Journal of Materials Chemistry A, 2018, 6, 7623-7630.	5.2	54
64	Cobalt-vanadium bimetal-based nanoplates for efficient overall water splitting. Science China Materials, 2018, 61, 80-90.	3.5	52
65	Cubic imidazolate frameworks-derived CoFe alloy nanoparticles-embedded N-doped graphitic carbon for discharging reaction of Zn-air battery. Science China Materials, 2020, 63, 327-338.	3.5	51
66	B,N-Doped Defective Carbon Entangled Fe ₃ C Nanoparticles as the Superior Oxygen Reduction Electrocatalyst for Zn–Air Batteries. ACS Sustainable Chemistry and Engineering, 2019, 7, 19104-19112.	3.2	48
67	Promising biomass-derived hierarchical porous carbon material for high performance supercapacitor. RSC Advances, 2017, 7, 10385-10390.	1.7	46
68	Porous Plate-like MoP Assembly as an Efficient pH-Universal Hydrogen Evolution Electrocatalyst. ACS Applied Materials & Interfaces, 2020, 12, 49596-49606.	4.0	46
69	TiO2-on-C3N4 double-shell microtubes: In-situ fabricated heterostructures toward enhanced photocatalytic hydrogen evolution. Journal of Colloid and Interface Science, 2020, 572, 22-30.	5.0	46
70	A novel Fe ₃ C/graphitic carbon composite with electromagnetic wave absorption properties in the C-band. RSC Advances, 2015, 5, 60135-60140.	1.7	45
71	Porous NiCoP nanowalls as promising electrode with high-area and mass capacitance for supercapacitors. Science China Materials, 2019, 62, 1115-1126.	3.5	42
72	A novel Ag/graphene composite: facile fabrication and enhanced antibacterial properties. Journal of Materials Science, 2013, 48, 1980-1985.	1.7	40

#	Article	IF	CITATIONS
73	In situ synthesis, enhanced luminescence and application in dye sensitized solar cells of Y2O3/Y2O2S:Eu3+ nanocomposites by reduction of Y2O3:Eu3+. Scientific Reports, 2016, 6, 37133.	1.6	38
74	Layer Stacked Iodine and Phosphorus Coâ€doped C ₃ N ₄ for Enhanced Visibleâ€Light Photocatalytic Hydrogen Evolution. ChemCatChem, 2017, 9, 4083-4089.	1.8	36
75	One-dimensional CO9S8-V3S4 heterojunctions as bifunctional electrocatalysts for highly efficient overall water splitting. Science China Materials, 2021, 64, 1396-1407.	3.5	36
76	Highly dispersed Ni-decorated porous hollow carbon nanofibers: fabrication, characterization, and NOx gas sensors at room temperature. Journal of Materials Chemistry, 2012, 22, 24814.	6.7	35
77	An effective "precursor-transformation―route toward the high-yield synthesis of ZIF-8 tubes. Chemical Communications, 2020, 56, 2913-2916.	2.2	35
78	ZnO-dotted porous ZnS cluster microspheres for high efficient, Pt-free photocatalytic hydrogen evolution. Scientific Reports, 2015, 5, 8858.	1.6	34
79	Ni ₂ P Entwined by Graphite Layers as a Low-Pt Electrocatalyst in Acidic Media for Oxygen Reduction. ACS Applied Materials & Interfaces, 2018, 10, 9999-10010.	4.0	34
80	N-doped carbon-coated Co3O4 nanosheet array/carbon cloth for stable rechargeable Zn-air batteries. Science China Materials, 2019, 62, 624-632.	3.5	34
81	Trace Pt Clusters Dispersed on SAPOâ€11 Promoting the Synergy of Metal Sites with Acid Sites for Highâ€Effective Hydroisomerization of <i>n</i> â€Alkanes. Small Methods, 2019, 3, 1800510.	4.6	34
82	2-D porous Ni ₃ N–Co ₃ N hybrids derived from ZIF-67/Ni(OH) ₂ sheets as a magnetically separable catalyst for hydrogenation reactions. Chemical Communications, 2018, 54, 11088-11091.	2.2	33
83	Hierarchical porous NiCo ₂ O ₄ nanosheet arrays directly grown on carbon cloth with superior lithium storage performance. Dalton Transactions, 2017, 46, 4717-4723.	1.6	32
84	Hollow CoP spheres assembled from porous nanosheets as high-rate and ultra-stable electrodes for advanced supercapacitors. Journal of Materials Chemistry A, 2021, 9, 26226-26235.	5.2	31
85	A "1-methylimidazole-fixation―route to anchor small-sized nitrides on carbon supports as non-Pt catalysts for the hydrogen evolution reaction. RSC Advances, 2016, 6, 29303-29307.	1.7	29
86	Electronic Structure Modulation of Nonâ€Nobleâ€Metalâ€Based Catalysts for Biomass Electrooxidation Reactions. Small Structures, 2021, 2, 2100095.	6.9	28
87	Fabrication of a 3D Hierarchical Flower‣ike MgO Microsphere and Its Application as Heterogeneous Catalyst. European Journal of Inorganic Chemistry, 2012, 2012, 954-960.	1.0	27
88	Single-step pyrolytic preparation of Mo2C/graphitic carbon nanocomposite as catalyst carrier for the direct liquid-feed fuel cells. RSC Advances, 2013, 3, 4771.	1.7	27
89	Synergistic Effect of Tungsten Nitride and Palladium for the Selective Hydrogenation of Cinnamaldehyde at the C=C bond. ChemCatChem, 2016, 8, 1718-1726.	1.8	26
90	A facile and green synthesis route towards two-dimensional TiO2@Ag heterojunction structure with enhanced visible light photocatalytic activity. CrystEngComm, 2013, 15, 5821.	1.3	25

#	Article	IF	CITATIONS
91	Twoâ€Dimensional Porous Molybdenum Phosphide/Nitride Heterojunction Nanosheets for pHâ€Universal Hydrogen Evolution Reaction. Angewandte Chemie, 2021, 133, 6747-6755.	1.6	25
92	Graphene-like nanocomposites anchored by Ni ₃ S ₂ slices for Li-ion storage. RSC Advances, 2016, 6, 48083-48088.	1.7	23
93	Self-supported Ni6MnO8 3D mesoporous nanosheet arrays with ultrahigh lithium storage properties and conversion mechanism by in-situ XAFS. Nano Research, 2017, 10, 263-275.	5.8	23
94	Promoting the spatial charge separation by building porous ZrO2@TiO2 heterostructure toward photocatalytic hydrogen evolution. Journal of Colloid and Interface Science, 2020, 561, 568-575.	5.0	23
95	Solvothermal Synthesis, Characterization, and Formation Mechanism of a Single‣ayer Anatase TiO ₂ Nanosheet with a Porous Structure. European Journal of Inorganic Chemistry, 2011, 2011, 754-760.	1.0	22
96	Surface curvature-confined strategy to ultrasmall nickel-molybdenum sulfide nanoflakes for highly efficient deep hydrodesulfurization. Nano Research, 2020, 13, 882-890.	5.8	22
97	Operando Cooperated Catalytic Mechanism of Atomically Dispersed Cuâ^'N 4 and Znâ^'N 4 for Promoting Oxygen Reduction Reaction. Angewandte Chemie, 2021, 133, 14124-14131.	1.6	22
98	Multi-touch cobalt phosphide-tungsten phosphide heterojunctions anchored on reduced graphene oxide boosting wide pH hydrogen evolution. Science China Materials, 2022, 65, 1225-1236.	3.5	21
99	Silica direct evaporation: a size-controlled approach to SiC/carbon nanosheet composites as Pt catalyst supports for superior methanol electrooxidation. Journal of Materials Chemistry A, 2015, 3, 24139-24147.	5.2	20
100	Znâ€Doped Porous CoNiP Nanosheet Arrays as Efficient and Stable Bifunctional Electrocatalysts for Overall Water Splitting. Energy Technology, 2020, 8, 1901079.	1.8	20
101	Oneâ€pot synthesis of silver particle aggregation as highly active SERS substrate. Journal of Raman Spectroscopy, 2011, 42, 5-11.	1.2	19
102	Facile synthesis and shape control of Fe3O4 nanocrystals with good dispersion and stabilization. CrystEngComm, 2013, 15, 3366.	1.3	19
103	Intermittent microwave heating-promoted rapid fabrication of sheet-like Ag assemblies and small-sized Ag particles and their use as co-catalyst of ZnO for enhanced photocatalysis. Journal of Materials Chemistry A, 2014, 2, 3015.	5.2	19
104	An effective poly(p-phenylenevinylene) polymer adhesion route toward three-dimensional nitrogen-doped carbon nanotube/reduced graphene oxide composite for direct electrocatalytic oxygen reduction. Nano Research, 2016, 9, 3364-3376.	5.8	19
105	A "competitive occupancy―strategy toward Co–N ₄ single-atom catalysts embedded in 2D TiN/rGO sheets for highly efficient and stable aromatic nitroreduction. Journal of Materials Chemistry A, 2020, 8, 4807-4815.	5.2	19
106	Ultrathin Porous Carbon Nitride Bundles with an Adjustable Energy Band Structure toward Simultaneous Solar Photocatalytic Water Splitting and Selective Phenylcarbinol Oxidation. Angewandte Chemie, 2021, 133, 4865-4872.	1.6	19
107	In Situ Reduction, Oxygen Etching, and Reduction Using Formic Acid: An Effective Strategy for Controllable Growth of Monodisperse Palladium Nanoparticles on Graphene. ChemPlusChem, 2012, 77, 301-307.	1.3	18
108	Gelatin-assisted synthesis of ZnS hollow nanospheres: the microstructure tuning, formation mechanism and application for Pt-free photocatalytic hydrogen production. CrystEngComm, 2017, 19, 461-468.	1.3	17

#	Article	IF	CITATIONS
109	Insight on the active sites of CoNi alloy embedded in N-doped carbon nanotubes for oxygen reduction reaction. Science China Materials, 2021, 64, 2719-2728.	3.5	16
110	Vanadiumâ€Incorporated CoP ₂ with Lattice Expansion for Highly Efficient Acidic Overall Water Splitting. Angewandte Chemie, 2022, 134, .	1.6	16
111	Heterojunction Ag–TiO ₂ Nanopillars for Visibleâ€Lightâ€Driven Photocatalytic H ₂ Production. ChemPlusChem, 2014, 79, 995-1000.	1.3	15
112	The Fe ₃ C–N _{<i>x</i>} Site Assists the Fe–N _{<i>x</i>} Site to Promote Activity of the Fe–N–C Electrocatalyst for Oxygen Reduction Reaction. ACS Sustainable Chemistry and Engineering, 2022, 10, 3346-3354.	3.2	15
113	A Platinum–Vanadium Nitride/Porous Graphitic Nanocarbon Composite as an Excellent Catalyst for the Oxygen Reduction Reaction. ChemElectroChem, 2015, 2, 1813-1820.	1.7	14
114	Graphitic Carbon Nanocapsules: Scaled Preparation, Formation Mechanism, and Use as an Excellent Support for Methanol Electro-oxidation. European Journal of Inorganic Chemistry, 2012, 2012, 961-968.	1.0	13
115	Confinement Effect on Ag Clusters in the Channels of Wellâ€Ordered Mesoporous TiO ₂ and their Enhanced Photocatalytic Performance. ChemCatChem, 2013, 5, 1354-1358.	1.8	13
116	A hybridized heterojunction structure between TiO2nanorods and exfoliated graphitic carbon-nitride sheets for hydrogen evolution under visible light. CrystEngComm, 2016, 18, 6875-6880.	1.3	13
117	Dyeâ€Sensitised Solar Cells Based on Largeâ€Pore Mesoporous TiO ₂ with Controllable Pore Diameters. European Journal of Inorganic Chemistry, 2011, 2011, 4730-4737.	1.0	12
118	A New Combustion Route to Synthesize Mixed Valence Vanadium Oxide Heterojunction Composites as Visibleâ€Lightâ€Driven Photocatalysts. ChemCatChem, 2014, 6, 2553-2559.	1.8	12
119	Constructing B and N separately co-doped carbon nanocapsules-wrapped Fe/Fe ₃ C for oxygen reduction reaction with high current density. Physical Chemistry Chemical Physics, 2016, 18, 26572-26578.	1.3	12
120	In situ intercalation and exploitation of Co3O4 nanoparticles grown on carbon nitride nanosheets for highly efficient degradation of methylene blue. Dalton Transactions, 2020, 49, 14665-14672.	1.6	12
121	Integration of heterointerface and porosity engineering to achieve efficient hydrogen evolution of 2D porous NiMoN nanobelts coupled with Ni particles. Electrochimica Acta, 2022, 403, 139702.	2.6	12
122	Moltenâ€Salt Technology Application for the Synthesis of Photocatalytic Materials. Energy Technology, 2021, 9, 2000945.	1.8	9
123	Ni-promoted MoS ₂ in hollow zeolite nanoreactors: enhanced catalytic activity and stability for deep hydrodesulfurization. Journal of Materials Chemistry A, 2022, 10, 7263-7270.	5.2	8
124	Clusterâ€like Co ₄ N embedded into carbon sphere as an efficient, magneticâ€separated catalyst for catalytic hydrogenation. ChemistrySelect, 2019, 4, 90-99.	0.7	7
125	2D thin sheets composed of Co _{5.47} N–MgO embedded in carbon as a durable catalyst for the reduction of aromatic nitro compounds. Materials Chemistry Frontiers, 2021, 5, 2798-2809.	3.2	7
126	Two-dimensional porous Cu-CuO nanosheets: Integration of heterojunction and morphology engineering to achieve high-effective and stable reduction of the aromatic nitro-compounds. Chinese Chemical Letters, 2023, 34, 107295.	4.8	7

#	Article	IF	CITATIONS
127	A general strategy toward the large-scale synthesis of the noble metal-oxide nanocrystal hybrids with intimate interfacial contact for the catalytic reduction of p-nitrophenol and photocatalytic degradation of pollutants. Research on Chemical Intermediates, 2017, 43, 4759-4779.	1.3	4
128	Cobalt nanoparticles decorated on nitrogen-doped graphene as excellent electromagnetic wave absorbent in Ku-band. Journal of Materials Science: Materials in Electronics, 2020, 31, 12044-12055.	1.1	4
129	Cobalt Nickel Nitrogen Array as a Easily Eecoverable, Effective Catalyst for Liquidâ€Phase Catalytic Reaction with Remarkable Recycled Stability. ChemistrySelect, 2019, 4, 3515-3523.	0.7	3
130	Facile immobilization of polyoxometalates for low-cost molybdenum/tungsten phosphide nanoparticles on carbon black for efficient electrocatalytic hydrogen evolution. Journal of Coordination Chemistry, 2020, 73, 2590-2601.	0.8	3
131	A Singleâ€Source Precursor Route toward Smallâ€Sized Nickel Particles Embedded into SiO 2 Sheet as Magnetic Separable Catalyst. ChemistrySelect, 2020, 5, 11708-11712.	0.7	1
132	Innenrücktitelbild: Ultrathin Porous Carbon Nitride Bundles with an Adjustable Energy Band Structure toward Simultaneous Solar Photocatalytic Water Splitting and Selective Phenylcarbinol Oxidation (Angew. Chem. 9/2021). Angewandte Chemie, 2021, 133, 5003-5003.	1.6	1